Tear-Film Evaporation Rate from Simultaneous Ocular-Surface Temperature and Tear-Breakup Area

Thomas J. Dursch, PhD,[1,2] Wing Li, OD, PhD,[2] Baseem Taraz, BS,[1] Meng C. Lin, OD, PhD, FAAO,[2,3] and Clayton J. Radke, PhD, NAE[1,2,3]*

SIGNIFICANCE: A corneal heat-transfer model is presented to quantify simultaneous measurements of fluorescein tear-breakup area (TBA) and ocular-surface temperature (OST). By accounting for disruption of the tear-film lipid layer (TFLL), we report evaporation rates through lipid-covered tear. The modified heat-transfer model provides new insights into evaporative dry eye.

PURPOSE: A quantitative analysis is presented to assess human aqueous tear evaporation rate (TER) through intact TFLLs from simultaneous *in vivo* measurement of time-dependent infrared OST and fluorescein TBA.

METHODS: We interpret simultaneous OST and TBA measurements using an extended heat-transfer model. We hypothesize that TBAs are ineffectively insulated by the TFLL and therefore exhibit higher TER than does that for a well-insulting TFLL-covered tear. As time proceeds, TBAs increase in number and size, thereby increasing the cornea area-averaged TER and decreasing OST. Tear-breakup areas were assessed from image analysis of fluorescein tear-film-breakup video recordings and are included in the heat-transfer description of OST.

RESULTS: Model-predicted OSTs agree well with clinical experiments. Percent reductions in TER of lipid-covered tear range from 50 to 95% of that for pure water, in good agreement with literature. The physical picture of noninsulating or ruptured TFLL spots followed by enhanced evaporation from underlying cooler tear-film ruptures is consistent with the evaporative-driven mechanism for local tear rupture.

CONCLUSIONS: A quantitative analysis is presented of *in vivo* TER from simultaneous clinical measurement of transient OST and TBA. The new heat-transfer model accounts for increased TER through expanding TBAs. Tear evaporation rate varies strongly across the cornea because lipid is effectively missing over tear-rupture troughs. The result is local faster evaporation compared with nonruptured, thick lipid–covered tear. Evaporative-driven tear-film ruptures deepen to a thickness where fluorescein quenching commences and local salinity rises to uncomfortable levels. Mitigation of tear-film rupture may therefore reduce dry eye–related symptoms.

Optom Vis Sci 2018;95:5–12. doi:10.1097/OPX.0000000000001156
Copyright © 2017 American Academy of Optometry
Supplemental Digital Content: *Direct URL links are provided within the text.*

SDC

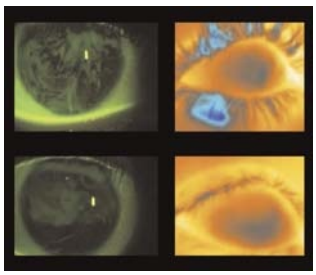

Author Affiliations:
[1]Chemical and Biomolecular Engineering Department, University of California, Berkeley, Berkeley, California
[2]Clinical Research Center, School of Optometry, University of California, Berkeley, Berkeley, California
[3]Vision Science Group, University of California, Berkeley, Berkeley, California
*radke@berkeley.edu

The human tear film provides lubrication and moisture necessary for clear vision and protection of the ocular surface. A thin tear-film lipid layer (~30 to 100 nm) covers thicker aqueous tear (~3 to 5 μm) and serves a key role in slowing evaporation.[1,2] Evaporative dry eye is associated with excessive tear-film evaporation that contributes to tear hyperosmolarity (e.g., > 600 to 800 mOsm).[3] Increased tear osmolarity leads to ocular discomfort through the activation of corneal nociceptors. Chronic activation potentially disrupts the corneal-lacrimal feedback loop, resulting in dry-eye symptoms.[3–6] Increased tear evaporation is also considered to be an important contributor to contact-lens wear discomfort.[7] Because of the significant role that aqueous tear-film evaporation plays in ocular-surface health, significant effort has been expended on developing a method to measure *in vivo* tear-film evaporation rates.[8–11]

Considerable research has focused on infrared thermography to measure transient ocular-surface temperature as a method to assess tear-film evaporation rates because the liquid-to-gas phase change during tear-film evaporation cools the ocular surface.[10–20] Although literature suggests correlation between ocular-surface temperature and tear-film evaporation rates,[10,11,13–15] no simple methodology exists to quantify tear-film evaporation rates from ocular-surface temperature data. Several authors have attempted to diagnose dry-eye disease by measuring the rate of ocular-surface temperature decline over time as a proxy for tear-film evaporation rates.[14,16] Unfortunately, this approach is flawed because transient ocular-surface temperature decline is not directly related to tear-film evaporation rates (described in Appendix A, http://links.lww.com/OPX/A326). We also demonstrate that tear-film evaporation rates are neither constant in time nor constant across the cornea. Further, tear-film evaporation rates and cooling rates depend strongly on environmental conditions such as ambient temperature, relative humidity, air circulation, and core body temperature.[17,18]

Recently, Tan et al.[11] developed a heat-transfer model to isolate the evaporative contribution to ocular-surface cooling and extract overall tear-film evaporation rates by considering the average ocular-surface temperature over the entire cornea. However, their model does not consider variations in local tear-film evaporation rates over regions of the tear film undergoing breakup.[11,19] The importance of corneal spatial variation in ocular-surface temperature is found in recent research establishing colocalization of fluorescein tear-film breakup areas and regions of enhanced cooling.[15,20] Fig. 1 shows representative sequential images of simultaneous tear-film breakup areas and ocular-surface temperature patterns from Li et al.[15] Left panels display transient growth of tear-rupture areas (black) under fluorescein instillation. Corresponding right panels demonstrate simultaneous growth of relatively cooler

Copyright © American Academy of Optometry. Unauthorized reproduction of this article is prohibited.

areas (darker regions). Cool areas grow in direct correlation with tear-rupture area growth. Li et al.[15] also report that cooling is observed 1 to 2 seconds before subsequent and coincident tear-film breakup area is observed. This result implies that spatial ocular-surface temperature gauges the active process of tear-film evaporation, whereas tear-film breakup area reflects local regions of the tear film thinned enough by evaporation to initiate blackness by fluorescence quenching.[21,22]

These observations coincide with the recent theory of Peng et al.,[2] arguing that prior tear-film lipid-layer disruption is a precondition for subsequent formation of tear-film breakup area.[23] Because the tear-film lipid layer inhibits aqueous evaporation by approximately 70 to 90%,[1,2,8,24,25] tear-film lipid-layer rupture spots cause locally elevated tear-film evaporation rates that open deepening fissures in the tear film.[8,15,25] These fissures appear as expanding black regions under fluorescein examination. Enhanced rates of evaporation through cooler lipid-free tear-film breakup areas contribute significantly to overall average tear-film evaporation rates. This phenomenon has been hypothesized previously[11–15,26] but not proven quantitatively.

We develop a quantitative model for *in vivo* tear-film evaporation rates through spatially varying lipid coverage of tear. An extended heat-transfer calculation is outlined to extract *in vivo* tear-film evaporation rate from combined ocular-surface temperature and tear-film breakup area data that accounts for tear-film lipid-layer disruption. The newly developed heat-transfer model is applied to ocular-surface temperature and tear-film breakup area data for nine subjects obtained via simultaneous infrared thermography and image analysis of fluorescein tear-film breakup measurements.[15] Physically realistic tear-film evaporation rates through intact tear-film lipid-layer regions are found only when enhanced aqueous tear evaporation through lipid-ruptured areas is accounted for.

METHODS

Subjects

Simultaneous measurement of transient ocular-surface temperature and tear-film breakup area was interpreted for nine subjects from Li et al.[15] Subjects were recruited from the University of California, Berkeley, and the surrounding community. Subjects taking systemic or ocular medication or with a history of ocular disease or surgery were excluded. No exclusion was made based on contact-lens wearing status, but subjects were asked to discontinue contact-lens wear for at least 24 hours prior to measurement. Subjects were instructed to refrain from applying eye makeup or eye drops on the day of the visit. Informed consent, with a complete description of the goals, risks, benefits, and procedures of the study, was obtained from all participants. This study observed the tenets of the Declaration of Helsinki and was approved by the University of California, Berkeley Committee for Protection of Human Subjects.

Ocular-Surface Temperature and Tear-film Breakup Area Measurement

As discussed in detail elsewhere,[15] transient ocular-surface temperatures were obtained using an FLIR A655sc (FLIR Systems, Wilsonville, OR) microbolometer infrared thermographer. A digital video camera (DXC390 3CCD Exwave HAD; Sony Electronics, Tokyo, Japan) was attached to a slit lamp to record tear-film breakup area.

In all cases, subjects were acclimated to the testing environment for 10 minutes.[15] Subject core temperatures were measured using an Exergen temporal artery thermometer (Exergen Corporation, Watertown, MA). Table 1 reports measured core temperatures for the nine subjects. Room temperature (24.8 ± 1.0°C) and

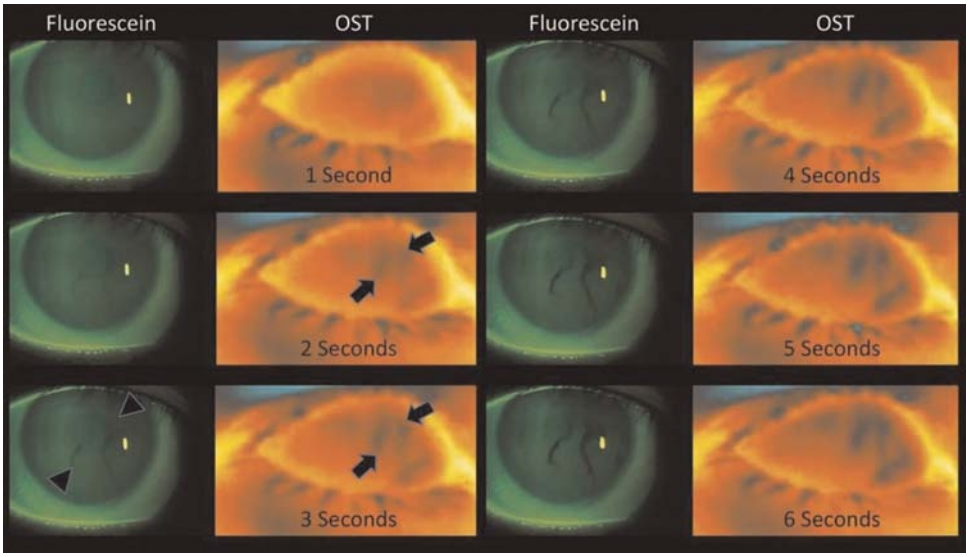

FIGURE 1. Correspondence of synchronized fluorescein tear breakup (left panels) and infrared thermography (right panels). Arrow tips demark areas of tear breakup, whereas arrows locate local cooling regions. Areas of cooling develop approximately 1 second before fluorescein tear breakup. Adapted with permission from Li et al.[15]

Copyright © American Academy of Optometry. Unauthorized reproduction of this article is prohibited.

TABLE 1. Subject parameters

Subject	T_B (°C)*	a (s^{-1})*	$\hat{J}_W \times 10^4$ ($kg/m^2/s$)*	β
1	36.7	0.030	1.95	0.24
2	36.8	0.045	1.84	0.50
3	37.1	0.057	1.78	0.38
4	36.9	0.049	1.88	0.33
5	36.7	0.063	1.82	0.05
6	36.6	0.016	1.79	0.50
7	36.8	0.033	1.87	0.44
8	36.6	0.019	1.95	0.02
9	36.8	0.062	1.86	0.07

*Obtained from independent experiments (see text and Appendix B, http://links.lww.com/OPX/A327).

relative humidity (near 50%) were recorded using a combination digital hygrometer and thermometer (DHT700; General Tools & Instruments, Secaucus, NJ).

A micropipette was used to instill 4 μL of 2% sodium fluorescein dye onto the superior bulbar conjunctiva of the right eye; subjects were asked to close and roll their eyes to distribute the dye evenly. Subjects were positioned in the slit lamp and instructed to blink five times and then to refrain from blinking while the digital video camera and infrared thermographer simultaneously interrogated the ocular surface. Fig. 1 illustrates typical results.

The FLIR+ Tools software suite (FLIR Systems) was used by an experienced observer (WL) to specify a defined region of interest corresponding to the cornea in the infrared recordings. The region represented 4000 to 7000 measurement points (accounting for anatomical variation), with the mean value of the points taken as the mean ocular-surface temperature.[15] Image-processing software (NI LabVIEW Vision Assistant 2012; National Instruments, Austin, TX) quantified tear-film breakup area over time during the interblink period using the method described elsewhere.[15]

Fig. 2 graphs resulting tear-film breakup areas from the video recordings (filled symbols), reported as a fraction of total cornea evaporation area, f_B, versus time, for three representative subjects. In all cases, area fraction increases roughly linearly with time following eye opening. As expected, the rate of area-fraction increase is subject dependent. In all cases, the rate of increase in area fraction slows somewhat at later time as the area fraction grows.

We follow Li et al.[15] and express the tear-film breakup area fraction in Fig. 2 as a straight line in time starting from time zero at eye opening

$$f_B(t) = at \qquad (1)$$

where a is the best eye-fit slope. Fig. 2 illustrates the straight-line fits, whereas Table 1 lists the resulting values of a for the nine subjects studied. Eq. 1 accounts for the finite time before initial tear breakup because of the threshold-luminance averaging utilized to capture tear-film breakup area.[27] More precise estimation of f_B demands correction for tear-breakup lag time. Fortunately, Eq. 1 gives a useful estimate of tear-film breakup area.

Fig. 3 graphs companion ocular-surface temperature versus time (filled symbols) for the three representative human subjects whose

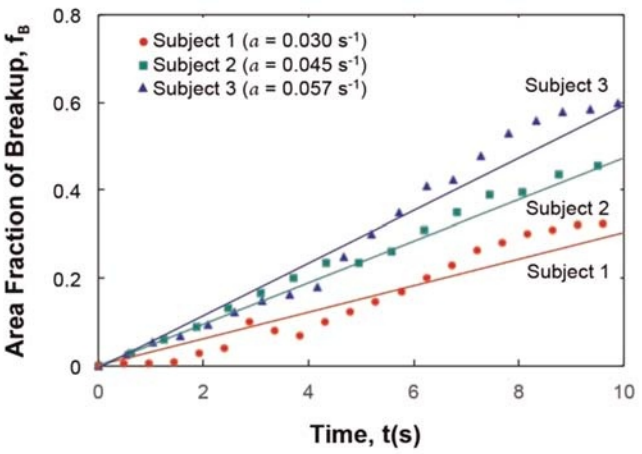

FIGURE 2. Tear-breakup area fraction, f_B, as a function of time after a blink for three typical subjects. Straight-line slopes a in Eq. 1 are listed.

corresponding tear-film breakup area fractions are exemplified in Fig. 2. In all cases, ocular-surface temperature decreases nonlinearly with time and to different final temperature asymptotes. In addition, each subject exhibits a different initial ocular-surface temperature that corresponds to a different body temperature, T_B (Table 1). Higher initial ocular-surface temperatures correspond to higher body temperatures.

Tear-Film Evaporation Rate Measurement

A physically based framework is required to ascertain tear-film evaporation rates from measurement of corneal-averaged ocular-surface temperatures and fluorescein tear-film breakup areas. Following others, we apply local conservation of energy.[11,28–30]

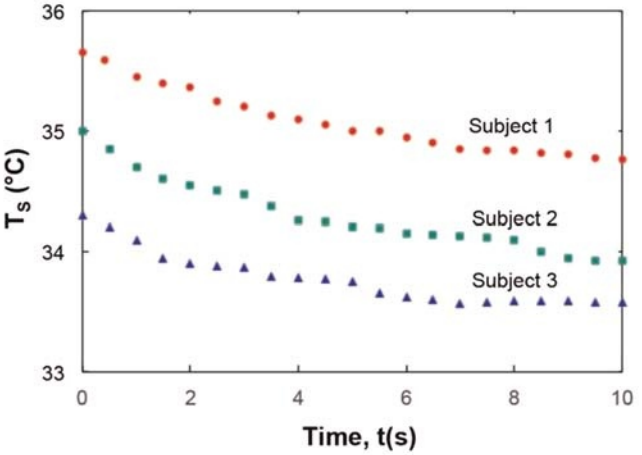

FIGURE 3. Measured ocular-surface temperatures as a function of time for the three subjects who tear-film breakup areas are displayed in Fig. 2. Each subject has a different initial ocular-surface temperature upon lid opening and consequently a different nonlinear temperature decline.

Copyright © American Academy of Optometry. Unauthorized reproduction of this article is prohibited.

Careful calculations of heat transfer in the eye evidence temperature profiles that decline from body temperature at the retina toward the preocular tear film.[28–30] Most of the eye-temperature decline, however, is sandwiched between the crystalline lens and the tear film.[10,11] To provide a convenient approach for quantifying tear-film evaporation rates, we lump the lens, anterior chamber, cornea, and tear film into a single composite cornea, as drawn in Fig. 4. Because typical ocular-surface temperatures are 1 to 2°C below body temperature, T_B, heat continually transfers from the back of the eye to the ocular surface (at $T_s(t)$).[11–14,28–30] Accordingly, as shown in Fig. 4 by $T_o(x)$, a closed-eye initial nonuniform temperature profile exists across the eye. Upon eye opening, the corneal surface temperature falls in time as the lower temperature environment and tear evaporation cool the eye. Appendix A, http://links.lww.com/OPX/A326, demonstrates that a one-dimensional analysis of transient eye cooling specifies the declining corneal surface temperature, $T_s(t)$ according to Eq. A8. The tear evaporation rate, $\hat{J}_E$ (in dimensions of mass loss per unit time per unit area), appears as a parameter in Eq. A8. Therefore, to obtain tear-film evaporation rate from clinical measurement of $T_s(t)$, the transient ocular-surface temperature data in Fig. 3 are best fit to Eq. A8 as outlined in Appendix A, http://links.lww.com/OPX/A326. Note that $\hat{J}_E$ in this specific analysis is a constant value averaged over the cornea.

Fig. 5 compares calculations from Eq. A8 to typical experimental ocular-surface temperatures in Fig. 3. Regions between solid curves are ocular-surface temperature predictions for a physically relevant range of $\hat{J}_E$ values between 10 and 20% of that for pure water (i.e., the values of $\hat{J}_W$ listed in Table 1).[1,2,8,24,25] Better fits to the ocular-surface temperature data in Fig. 5 can be obtained if $\hat{J}_E$ is set to almost the value for pure water.

We reject the possibility of pure-water evaporation rates for several reasons. First, for a typical tear-film thickness of 3 μm and an evaporation rate of pure water, the tear film disappears within a 5-second interblink exposing bare cornea. Second, direct measurements of human tear evaporation rate,[8,9,31,32] including the most recent by Peng et al.,[8] quantitatively confirm the accepted view that the lipid layer provides an important thermal barrier to tear evaporation, upward of 70 to 95% reductions in water evaporation rate. Third, and most important, a constant tear evaporation rate is inconsistent with the findings in Fig. 1 that ocular-surface temperature is distributed nonuniformly across the cornea. Rather, ocular-surface temperature is colder over breakup areas, signifying high evaporation rates, and warmer outside those areas, signifying lower evaporation rates. Accordingly, we impose the limitation that reductions in tear evaporation are significant when the tear-film lipid layer thermally insulates effectively. This limitation is imposed in the regions of Fig. 5 between the solid curves.

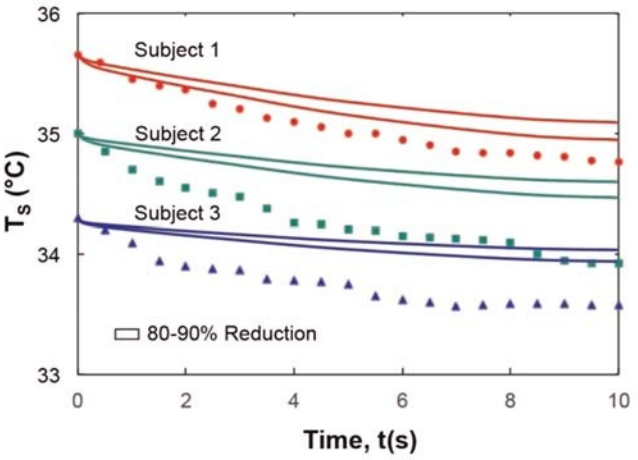

FIGURE 5. Comparison of measured and calculated (from Eq. A8) ocular-surface temperature as a function of time for three subjects whose tear-film breakup area fractions are graphed in Fig. 2. Regions between solid curves correspond to predicted homogeneous 80 to 90% reductions in evaporation rate compared with that of pure water evaluated at $T_S(0)$ for a given subject.

Deviation of experiment from theory presented in Fig. 5 starts early on and worsens in time for all three subjects. Especially apparent is the stark disagreement between experimental and predicted final steady-state ocular-surface temperature, suggesting significant underestimation of tear-film evaporation rate at longer times.

Clearly in Figs. 3 and 5, ocular-surface temperature does not fall linearly in time and therefore does not exhibit a constant

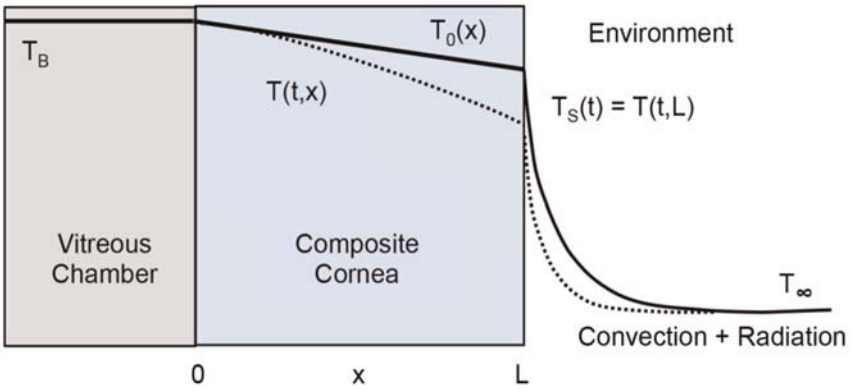

FIGURE 4. Schematic of the transient temperature profile (dashed line) through the eye from the vitreous humor, T_B, to the ocular surface, T_S, and into the environment, T_∞. Temperature is relatively uniform behind the crystalline lens.[28,29] $T_o(x)$ is the initial nonuniform temperature profile (solid line) through the composite cornea prior to lid opening. The temperature profile in the environment is qualitative.

Copyright © American Academy of Optometry. Unauthorized reproduction of this article is prohibited.

ocular-surface cooling rate.[14–16] Even at early times, a linear decline in ocular-surface temperature is not correct. Importantly, Fig. 5 reveals that Eq. A8 (solid curves) does not correctly reflect measured ocular-surface temperature data. Apparently, the assumption that $\hat{J}_E$ is constant is inadequate. Our explanation for the disagreement from theory in Fig. 5 emerges from examination of Fig. 1 that demonstrates nonuniform ocular-surface temperature distribution across the cornea. In particular, cooler (darker) corneal regions are observed over tear-film breakup areas, corresponding to disruption of the tear film.[15] During an interblink, cooler tear-film breakup areas increase in size and number, further reducing area-averaged ocular-surface temperature.

Peng et al.[2] assert that tear-film breakup areas correspond to evaporative tear rupture under lipid-ineffective tear regions. Without a well-insulating lipid covering, tear evaporation through black spots/streaks is fast, close to that of pure water, compared with that through the remaining areas effectively insulated by lipid. Tear-film breakup areas are therefore cooler, consistent with Fig. 1.[2,15] To account for this observation, we express the total cornea tear-film evaporation rate as the area-weighted average through lipid-ineffective and well-insulating lipid-coated regions or

$$\hat{J}_E(t) = \hat{J}_W f_B(t) + \beta \hat{J}_W [1 - f_B(t)] \qquad (2)$$

where $\hat{J}_W$ is the evaporation rate through lipid-disrupted tear-breakup areas, estimated as that of pure water, and $\beta\hat{J}_W$ is the evaporation rate of tear through intact-tear lipid-covered areas of the corneal surface, where β is the fraction of pure-water evaporation rate due to the resistance of an intact tear-film lipid layer. Alternately, 1-β is the fraction reduction of pure-water evaporation rate by a well-insulating tear-film lipid layer. Eq. 2 demands that tear-film evaporation rate is not a constant characteristic of a given subject in a specified environment. Rather, tear-film evaporation rate increases in time as more tear-film breakup areas appear and grow. That is, f_B in Eq. 2 increases in time. Only with a nonruptured/effective-insulating tear-film lipid layer is tear-film evaporation rate a constant in a given external environment.

The increasing tear-film evaporation rate with time in Eq. 2 explains the overestimation of ocular-surface temperature decline from Eq. A8 observed in Fig. 5. At early time, tear-film evaporation rate occurs slowly through a well-insulating, protective lipid layer before any tear-film breakup areas form (i.e., $f_B \sim 0$). Later, poorly insulating/ruptured tear-film lipid-layer areas appear and expand; tear-film evaporation rate increases. A lower average ocular-surface temperature emerges. Cooler expanding black areas in Fig. 1 need not be completely devoid of lipid covering. However, it is requisite that the evaporation rate through the anterior tear surface over expanding tear ruptures is faster than that over the nonruptured tear film. That is, complete lipid-layer rupture is a sufficient but not necessary criterion to explain evaporative-driven tear rupture.

Eqs. 2 and A8 are solved numerically as described in Appendix A, http://links.lww.com/OPX/A326. Four parameters appear in the analysis: $\hat{J}_W$, the evaporation rate of pure water; h_{eff}, the effective environmental heat-transfer coefficient; a, the slope of the tear-breakup area kinetics; and β, the ratio of tear-film evaporation rate to that of pure water. As described in Appendix B (http://links.lww.com/OPX/A327), $\hat{J}_W$ and h_{eff} are measured from separate *in vitro* water-evaporation experiments; a is determined experimentally for each subject from measured tear-breakup areas, as illustrated in Fig. 2 (Table 1); β, the only unknown parameter, is obtained by best fit of Eqs. 2 and A8 to the measured dynamic ocular-surface temperatures in Fig. 3. Appendix A discusses the procedure.

Incorporation of Eq. 2 into Eq. A8 is not rigorous. Strictly, Eq. A8 holds for constant parameters, whereas we allow $\hat{J}_E$ to vary with time according to Eq. 2. Rigorous solution to Eqs. 2 and A8 requires a fully three-dimensional transient energy balance in place of Eq. A1. Subsequent analysis to obtain tear-film evaporation rate from measured ocular-surface temperature and tear-film breakup area then is overly complicated and impractical.

RESULTS

Solid lines in Fig. 6 correspond to best fits to obtain β (the fraction of pure-water evaporation rate due to the resistance of an intact tear-film lipid-layer coating) from Eq. 2 and A8 for the same three subjects in Figs. 3 and 5. Modified heat-transfer theory now shows excellent agreement with the experiment. The reason for the discrepancies of the unmodified theory in Fig. 5 is the increased tear-film evaporation rate at longer times due to poor insulation of the protective lipid layer over growing tear-film breakup areas of the tear film. A well-insulating lipid layer reduces tear-film evaporation rate significantly, but only in those areas of the tear film where it remains effective. For the three subjects in Figs. 3, 5, and 6, β varies between 0.5 and 0.24, indicating a 50 to 76% reduction, respectively, in the evaporation rate of pure water when aqueous tear is covered by a well-functioning tear-film lipid layer.

Fig. 7 summarizes the obtained evaporation rates of lipid-coated tear for the nine subjects in terms of 1-β, the fractional reduction of the evaporation rate of pure water. Tear-film evaporation rates range from 10^{-6} to 10^{-5} g/cm^2/s or 95 to 50% reduction from that of pure water. Flow-evaporimeter measurements give average tear-film evaporation rates of approximately 4×10^{-6} g/cm^2/s,[8] in reasonable agreement with those determined here by ocular-surface temperature measurements. Accounting for local increases in tear-film evaporation rates due to tear-film breakup is critical to

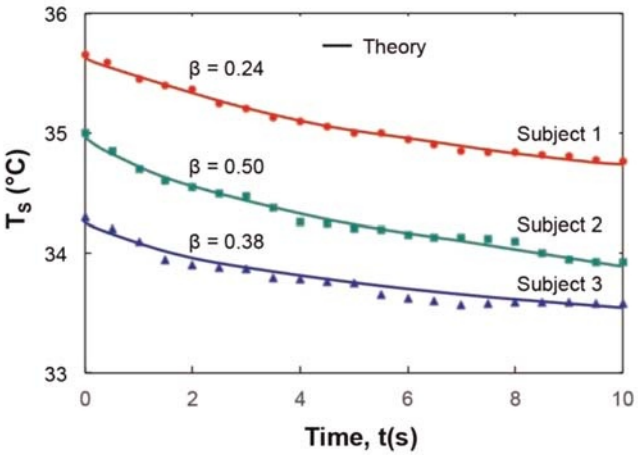

FIGURE 6. Comparison of experimental ocular-surface temperature as a function of time (symbols) to proposed theory from Eqs. 2 and A8 for three typical subjects. Solid lines correspond to best fits for β.

Copyright © American Academy of Optometry. Unauthorized reproduction of this article is prohibited.

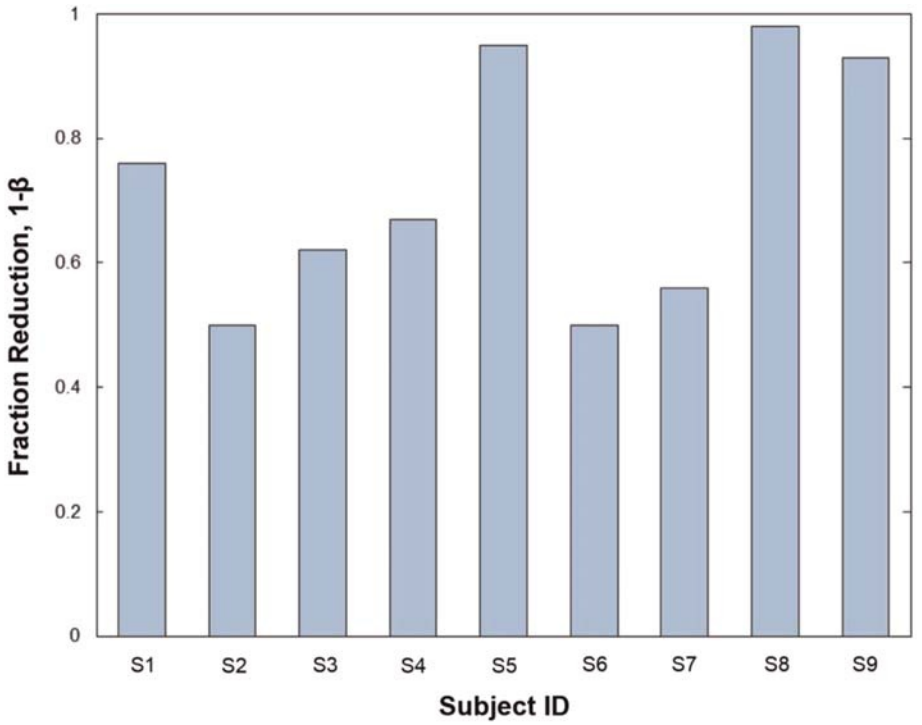

FIGURE 7. Tear evaporation rate through intact lipid layer for nine subjects reported as 1-β, the fraction reduction compared with pure water evaluated at $T_S(0)$ for each subject, according to the lipid-breakup heat-transfer model in Eqs. 2 and A8.

obtain reliable *in vivo* tear-film evaporation rates from ocular-surface temperature experiments.

DISCUSSION

Simultaneous measurement of transient tear-film breakup area and ocular-surface temperature and analysis indicate that lipid-layer evaporative disruption precedes and colocalizes with tear breakup.[15,20] Lipid-layer disruption either by local rupture or by local noninsulating thickness/composition change is apparently a prerequisite for subsequent localized tear rupture.[2] Once the tear-film lipid layer locally thins or breaks,[2,33] its protective role against tear evaporation diminishes. Enhanced tear-film evaporation rate through lipid-ineffective or lipid-free areas leads to observable tear-film breakup areas when the underlying tear-film rupture troughs thin enough for fluorescein quenching.[21,22,33] Tear-film evaporation rates are not constant either spatially or temporally. They commonly vary across the cornea during the interblink,[11,19] but even more so because the tear-film lipid layer is not uniform. Augmented evaporation through tear-film breakup areas explains why those regions are cooler than the surrounding warmer well-insulating lipid-covered regions and why the average tear-film evaporation rate increases with increasing tear-film breakup area. Only by incorporating local ineffective tear-film lipid-layer distribution with enhanced tear-film evaporation rate can our ocular-surface temperature measurements be properly interpreted and quantified. All evaporation measurements to date[8,9,31,32,34–36] report a time and spatially averaged rate. Not accounting for ineffective lipid-layer insulation in the averaged measurements underestimates the elevated tear-film evaporation rate in those localized regions, which is a major driver for evaporative dry-eye symptoms.[3,5,37]

Another potentially important insight on evaporative dry eye is gleaned from our extended heat-transfer model: it permits assessment of the tear-film evaporation rate through intact tear-film lipid layer, not an average value through both lipid-ineffective and lipid-insulated tear. For the nine subjects studied, an effective tear-film lipid layer reduces tear-film evaporation rate by 50 to 95% (i.e., a 2- to 20-fold reduction) when compared with pure water, in line with generally accepted values.[1,8,24,25,38] Intersubject variability of tear-film evaporation rate reduction by the tear-film lipid layer is likely mediated by a combination of factors including tear-film lipid-layer composition,[39] thickness,[40] and organization.[41] Even with a uniformly coated lipid layer, however, relatively high tear osmolarity can still occur, albeit not as high. For example, a stable tear film covered by homogeneous lipid layer offering 50% tear-film evaporation rate reduction makes the ocular surface more susceptible to a higher tear osmolarity than that afforded by a 95% lipid-layer evaporation rate reduction with nearly up to 50% tear-film rupture. Accordingly, tear-film instability is not an unassailable diagnostic for meibomian gland dysfunction.[37] Tear hyperosmolarity can still occur in the absence of lipid-layer rupture if the intact tear-film lipid layer is poor at inhibiting tear evaporation.[42,43] Most importantly, an evaporative-ineffective lipid layer may explain why patients who present long tear-breakup times or who blink frequently, which theoretically prevents tear-film lipid-layer rupture, may yet be susceptible to evaporative dry eye. Because the subjects studied here were not prescreened for dye-eye symptoms, additional work is needed to understand the etiology of tear-film evaporation rate reduction by an intact tear-film lipid

Copyright © American Academy of Optometry. Unauthorized reproduction of this article is prohibited.

layer and the importance of tear-film lipid-layer rupture in evaporative dry eye and contact-lens discomfort.

Simultaneous ocular-surface temperature and tear-film breakup area data[15,20] re-enforce the physical picture of lipid-initiated evaporative tear-film breakup first enunciated by Peng et al.[2] Once the thin tear-film lipid layer locally loses barrier effectiveness, a cascade of events follows: local enhanced tear evaporation and cooling, local tear thinning to fluorescein quenching and blackness in spots and streaks, and local increased salt concentrations. Local osmolarity in tear-film breakup areas is high enough to cause discomfort and contribute to dry-eye symptoms.[2,3] Nevertheless, the range of tear-film evaporation rate reduction observed for homogeneous, intact tear-film lipid layers argues that it is important to understand not only the propensity of tear-film lipid layer to rupture, but also the properties that mediate lipid-layer evaporation rate reduction.[2,42,44] Therefore, prevention of evaporative dry-eye discomfort points to stabilizing the tear film against rupture and to improving the ability of the tear-film lipid layer to reduce tear-film evaporation rate.[45]

ARTICLE INFORMATION

Supplemental Digital Content: Appendix A: Ocular-Surface Temperature Physical Model. Appendix A, available at http://links.lww.com/OPX/A326, outlines the modified heat-transfer theory necessary to interpret the ocular-surface temperature clinical data.

Appendix B: In-vitro Measurement of the Effective Heat Transfer Coefficient. Appendix B, available at http://links.lww.com/OPX/A327, presents measurements of the heat-transfer parameters necessary to apply theory to the measured ocular-surface-temperature clinical data.

Submitted: April 28, 2017

Accepted: October 27, 2017

Funding/Support: None of the authors have reported funding/support.

Conflict of Interest Disclosure: None of the authors have reported a conflict of interest.

Author Contributions and Acknowledgments: Conceptualization; Formal Analysis, Investigation, Methodology, Supervision, Writing – Original Draft, Writing – Review & Editing: CJR; Investigation, Methodology: TJD, WL, BT, MCL.

The authors thank Daniel Bergante for help with the *in vitro* evaporation-rate measurements.

REFERENCES

1. Craig JP, Tomlinson A. Importance of the Lipid Layer in Human Tear Film Stability and Evaporation. Optom Vis Sci 1997;74:8–13.

2. Peng CC, Cerretani C, Braun RJ, et al. Evaporation-driven Instability of the Precorneal Tear Film. Adv Colloid Interface Sci 2013;206:1–15.

3. Liu H, Begley C, Chen M, et al. A Link between Tear Instability and Hyperosmolarity in Dry Eye. Invest Ophthalmol Vis Sci 2009;50:3671–9.

4. Rosenthal P, Baran I, Jacobs DS. Corneal Pain without Stain: Is It Real? Ocul Surf 2009;7:28–40.

5. Ji RR, Woolf CJ. Neuronal Plasticity and Signal Transduction in Nociceptive Neurons: Implications for the Initiation and Maintenance of Pathological Pain. Neurobiol Dis 2001;8:1–10.

6. Hirata H, Mizerska K, Dallacasagrande V, et al. Estimating the Osmolarities of Tears during Evaporation through the "Eyes" of the Corneal Nerves. Invest Ophthalmol Vis Sci 2017;58:168–78.

7. Craig JP, Willcox MD, Argüeso P, et al. The TFOS International Workshop on Contact Lens Discomfort: Report of the Contact Lens Interactions with the Tear Film Subcommittee. Invest Ophthalmol Vis Sci 2013;54:TFOS123–56.

8. Peng CC, Cerretani CF, Li Y, et al. Flow Evaporimeter to Assess Evaporative Resistance of Human Tear-Film Lipid Layer. Ind Eng Chem Res 2014;53:18130–9.

9. Rolando M, Refojo MF. Tear Evaporimeter for Measuring Water Evaporation Rate from the Tear Film under Controlled Conditions in Humans. Exp Eye Res 1983;36:25–33.

10. Purslow C, Wolffsohn JS. Ocular Surface Temperature: A Review. Eye Contact Lens 2005;31:117–23.

11. Tan JH, Ng EYK, Acharya UR. Evaluation of Tear Evaporation from Ocular Surface by Functional Infrared Thermography. Med Phys 2010;37:6022–34.

12. Purslow C, Wolffsohn JS, Santodomingo-Rubido J. The Effect of Contact Lens Wear on Dynamic Ocular Surface Temperature. Cont Lens Anterior Eye 2005;28:29–36.

13. Craig JP, Singh I, Tomlinson A, et al. The Role of Tear Physiology in Ocular Surface Temperature. Eye 2000;14:635–41.

14. Morgan PB, Tull AB, Efron N. Ocular Surface Cooling in Dry Eye—A Pilot Study. J Br Contact Lens 1996;19:7–10.

15. Li W, Graham AD, Lin MC. Ocular Surface Cooling Corresponds to Tear Film Thinning and Breakup. Optom Vis Sci 2015;92:e248–56.

16. Fujishima H, Toda I, Yamada M, et al. Corneal Temperature in Patients with Dry Eye Evaluated by Infrared Radiation Thermometry. Br J Ophthalmol 1996;80:29–32.

17. Kessel L, Johnson L, Arvidsson H, et al. The Relationship between Body and Ambient Temperature and Corneal Temperature. Invest Ophthalmol Vis Sci 2010;51:6593–7.

18. Freeman RD, Fatt I. Environmental Influences on Ocular Temperature. Invest Ophthalmol 1973;12:596–602.

19. Tan JH, Ng E, Rajendra Acharya U, et al. Infrared Thermography on Ocular Surface Temperature: A Review. Infrared Phys Technol 2009;52:97–108.

20. Su TY, Chang SW, Yang CJ, et al. Direct Observation and Validation of Fluorescein Tear Film Break-up Patterns by Using a Dual Thermal-Fluorescent Imaging System. Biomed Opt Express 2014;5:2614–9.

21. Braun RJ, Gewecke NR, Begley CG, et al. A Model for Tear Film Thinning with Osmolarity and Fluorescein. Invest Ophthalmol Vis Sci 2014;55:1133–42.

22. Nichols JJ, King-Smith PE, Hinel EA, et al. The Use of Fluorescent Quenching in Studying the Contribution of Evaporation to Tear Thinning. Invest Ophthalmol Vis Sci 2012;53:5426–32.

23. King-Smith PE, Reuter KS, Braun RJ, et al. Tear Film Breakup and Structure Studied by Simultaneous Video Recording of Fluorescence and Tear Film Lipid Layer Images. Invest Ophthalmol Vis Sci 2013;54:4900–9.

24. Iwata S, Lemp MA, Holly FJ, et al. Evaporation Rate of Water from the Precorneal Tear Film and Cornea in the Rabbit. Invest Opthalmol Vis Sci 1969;8:613–9.

25. Cerretani CF, Ho NH, Radke CJ. Water-Evaporation Reduction by Duplex Films: Application to the Human Tear Film. Adv Colloid Interface Sci 2013;197–198:33–57.

26. Kimball SH, King-Smith PE, Nichols JJ. Evidence for the Major Contribution of Evaporation to Tear Film Thinning between Blinks. Invest Ophthalmol Vis Sci 2010;51:6294–7.

27. Begley C, Himebaugh N. Tear Breakup Dynamics: A Technique for Quantifying Tear Film Instability. Optom Vis Sci 2006;83:15–21.

28. Ooi EH, Ng E. Effects of Natural Convection within the Anterior Chamber on the Ocular Heat Transfer. Int J Numer Meth Bio 2011;27:408–23.

29. Ooi EH, Ng E. Ocular Temperature Distribution: A Mathematical Perspective. J Mech Med Biol 2009;9:199–227.

30. Ooi EH, Ng E. Simulation of Aqueous Humor Hydrodynamics in Human Eye Heat Transfer. Comput Biol Med 2008;38:252–62.

31. Goto E, Endo K, Suzuki A, et al. Tear Evaporation Dynamics in Normal Subjects and Subjects with Obstructive Meibomian Gland Dysfunction. Invest Ophthalmol Vis Sci 2003;44:533–9.

32. Mathers W. Evaporation from the Ocular Surface. Exp Eye Res 2004;78:389–94.

33. King-Smith PE, Ramamoorthy P, Braun RJ, et al. Tear Film Images and Breakup Analyzed Using Fluorescent Quenching. Invest Ophthalmol Vis Sci 2013;54:6003–11.

34. Arciniega JC, Wojtowicz JC, Mohamed EM, et al. Changes in the Evaporation Rate of Tear Film After

Copyright © American Academy of Optometry. Unauthorized reproduction of this article is prohibited.

Digital Expression of Meibomian Glands in Patients with and without Dry Eye. Cornea 2011;30:843–7.

35. Tsubota K, Yamada M. Tear Evaporation from the Ocular Surface. Invest Ophthalmol Vis Sci 1992;33:2942–50.

36. Khanal S, Tomlinson A, Diaper CJ. Tear Physiology of Aqueous Deficiency and Evaporative Dry Eye. Optom Vis Sci 2009;86:1235–40.

37. Knop E, Knop N, Millar T, et al. The International Workshop on Meibomian Gland Dysfunction: Report of the Subcommittee on Anatomy, Physiology, and Pathophysiology of the Meibomian Gland. Invest Ophthalmol Vis Sci 2011;52:1938–78.

38. King-Smith PE, Bailey MD, Braun RJ. Four Characteristics and a Model of an Effective Tear Film Lipid Layer (TFLL). Ocul Surf 2013;11:236–45.

39. Pucker AD, Nichols JJ. Analysis of Meibum and Tear Lipids. Ocul Surf 2012;10:230–50.

40. King-Smith PE, Nichols JJ, Braun RJ, et al. High Resolution Microscopy of the Lipid Layer of the Tear Film. Ocul Surf 2011;9:197–211.

41. Leiske DL, Miller CE, Rosenfeld L, et al. Molecular Structure of Interfacial Human Meibum Films. Langmuir 2012;28:11858–65.

42. Cerretani CF, Radke CJ. Tear Dynamics in Healthy and Dry Eyes. Curr Eye Res 2014;39:580–95.

43. Viitala T, Kulovesi P, Telenius J, et al. Molecular Organization of the Tear Fluid Lipid Layer. Biophys J 2010;99:2559–67.

44. Begley C, Simpson T, Liu H, et al. Quantitative Analysis of Tear Film Fluorescence and Discomfort during Tear Film Instability and Thinning. Invest Ophthalmol Vis Sci 2013;54:2645–53.

45. Svitova TF, Lin MC. Dynamic Interfacial Properties of Human Tear-Lipid Films and Their Interactions with Model-Tear Proteins *in Vitro*. Adv Colloid Interface Sci 2016;233:4–24.

Copyright © American Academy of Optometry. Unauthorized reproduction of this article is prohibited.